THE JOURNAL OF BIOLOGICAL CHEMISTRY VOL. 287, NO. 20, pp. 16645–16655, May 11, 2012

Calmodulin and S100A1 Protein Interact with N Terminus of TRPM3 Channel*[S]

Received for publication, February 8, 2012, and in revised form, March 26, 2012 Published, JBC Papers in Press, March 26, 2012, DOI 10.1074/jbc.M112.350686

Blanka Holakovska[‡], Lenka Grycova[‡], Michaela Jirku[‡], Miroslav Sulc[§], Ladislav Bumba[§], and Jan Teisinger[‡1]

From the [‡]Institute of Physiology and [§]Institute of Microbiology, Academy of Sciences of the Czech Republic, Videnska 1083, 142 20 Prague, Czech Republic

Background: Calcium-binding proteins bind to intracellular termini of TRP channels.
Results: Two Ca^{2+}-dependent binding sites for CaM/S100A1 were revealed by biophysical methods on TRPM3 N terminus.
Conclusion: CaM and S100A1 serve as ligands for TRPM3 channel.
Significance: Two clusters of positively charged residues form mutual binding sites for CaM and S100A1 proteins on TRPM3 N terminus.

Transient receptor potential melastatin 3 ion channel (TRPM3) belongs to the TRP family of cation-permeable ion channels involved in many important biological functions such as pain transduction, thermosensation, and mechanoregulation. The channel was reported to play an important role in Ca^{2+} homeostasis, but its gating mechanisms, functions, and regulation are still under research. Utilizing biophysical and biochemical methods, we characterized two independent domains, Ala-35–Lys-124 and His-291–Gly-382, on the TRPM3 N terminus, responsible for interactions with the Ca^{2+}-binding proteins calmodulin (CaM) and S100A1. We identified several positively charged residues within these domains as having a crucial impact on CaM/S100A1 binding. The data also suggest that the interaction is calcium-dependent. We also performed competition assays, which suggested that CaM and S100A1 are able to compete for the same binding sites within the TRPM3 N terminus. This is the first time that such an interaction has been shown for TRP family members.

The transient receptor potential melastatin 3 (TRPM3) ion channel is a member of the melastatin TRP[2] subfamily. It is closely related to the first known member of the TRPM subfamily, TRPM1 (1). TRPM3 shares typical structural features with other TRP family members, such as six putative transmembrane-spanning domains, intracellular N and C termini, and a conserved TRP box and coiled-coil region in its C terminus (2, 3). There are no ankyrin repeat domains present on its N-tail; instead, there is a so-called TRPM homology region, a roughly 700-amino acid-long domain only found in TRPM family members (4).

The channel is proposed to mediate a Ca^{2+} concentration-dependent Ca^{2+} entry pathway in kidney cells and thus is thought to play an important role in renal Ca^{2+} homeostasis (2, 5). Recently, TRPM3 was also reported to serve as a nociceptor channel involved in the detection of noxious heat (6).

Calcium entry pathways make TRPM3 a probable target for Ca^{2+}-binding proteins such as calmodulin and S100 proteins. Calmodulin (CaM) is a small cytoplasmic protein (16.7 kDa) that is ubiquitously expressed in all eukaryotic organisms. It contains four EF-hand motifs that bind Ca^{2+} ions cooperatively. When binding Ca^{2+}, CaM undergoes a conformational change that increases its affinity for its target proteins (7). CaM was found to regulate the function of numerous TRP channels via binding to their intracellular termini. Multiple CaM binding sites were reported on either the N-tail or the C-tail of TRPC, TRPV, and TRPM ion channel family members (7–10). These domains conform to at least one of the consensus CaM recognition motifs 1-5-10 or 1-8-14 and often contain more than one of these binding motifs (7–10).

The S100 proteins are a group of proteins with at least 25 members found in humans. Most of these proteins bind calcium and undergo a conformational change enabling them to interact with specific target proteins and control cellular activity (11). The proteins contain two EF-hand calcium binding domains, and in contrast to CaM, the first EF-hand motif binds Ca^{2+} with a lower affinity than the second EF-hand (12, 13). S100 proteins have been shown to bind similar structural motifs to CaM (14), and the Ca^{2+}-S100A1 complex also interacts with target proteins via a Ca^{2+}-dependent mechanism to elicit biological responses. One of the first characterized proteins of this family was S100A1. It is a small (10.5-kDa) protein that forms dimers containing four EF-hand Ca^{2+} binding motifs.

Here we show that CaM and S100A1 bind to the N terminus of the TRPM subfamily. Using two recombinant protein constructs corresponding to the TRPM3 sequences 35–124 and 291–382, we were able to find CaM/S100A1 binding sites using a combination of biophysical and bioinformatical tools. Furthermore, we proved that these two Ca^{2+}-binding proteins compete for these binding sites. Our results suggest that CaM

* This study was supported by the Grant Agency of the Czech Republic (Grants GACR 301/10/1159, GACR P205/10/P308, and GACR 207/11/0717) and the Academy of Sciences of the Czech Republic (Research Project AV0Z50110509).
[S] This article contains supplemental Figs. 1–3.
[1] To whom correspondence should be addressed: Dept. of Protein Structures, Institute of Physiology, Academy of Sciences of the Czech Republic, Videnska 1083, 142 20 Prague, Czech Republic. Tel.: 420-241062740; Fax: 420-241064447; E-mail: teisingr@biomed.cas.cz.
[2] The abbreviations used are: TRP, transient receptor potential; TRPM, transient receptor potential melastatin; TRPC, transient receptor potential canonical; TRPV, transient receptor potential vanilloid; CaM, calmodulin; DNS, dansyl chloride; SPR, surface plasmon resonance; CaV, voltage-gated calcium channel.

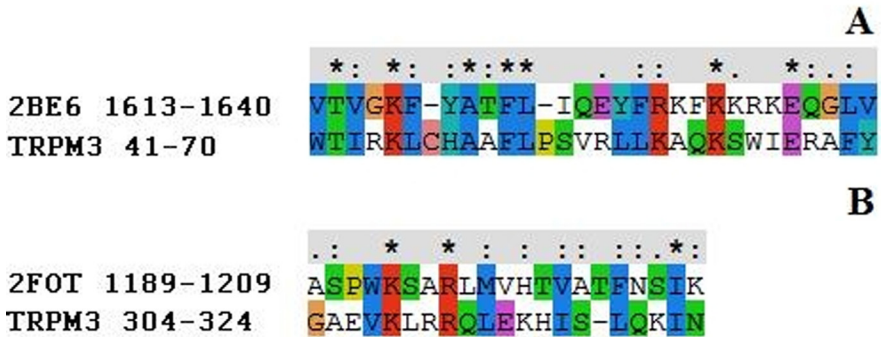

FIGURE 1. **Sequence alignment of TRPM3 N terminus 41–70 (*A*) and 304–324 (*B*) with their templates voltage-gated calcium channel CaV1.2 IQ domain (PDB code 2be6) and αII-spectrin (PDB code 2fot), respectively.** Identical amino acids are marked with an *asterisk*, similar amino acids with the more important groups are indicated with a *colon*, and *dots* indicate similar amino acids of the less important groups that are less likely to influence the protein structure.

and S100A1 serve as important regulators of TRPM3, which is known to play an important role in Ca^{2+} homeostasis. Whether CaM and S100A1 act as activators, inhibitors, or bidirectional regulators still remains elusive and will require further investigation.

EXPERIMENTAL PROCEDURES

Cloning and Site-directed Mutagenesis of Protein Constructs on N terminus of Human TRPM3—The N-terminal sequence of human TRPM3 was analyzed for a presence of potential CaM binding motifs with the Calmodulin Target Database (15). Based on this analysis, two putative CaM binding domains were found, Ala-35–Lys-124 ($TRPM3_{35-124}$) and His-291–Gly-382 ($TRPM3_{291-382}$). cDNA from the human TRPM3 N terminus corresponding to these sequences was cloned into the bacterial expression vector pET32b (Novagen). Using the QuikChange (Stratagene) method, point mutations were created in both N-terminal protein constructs. The integrity of the coding region and the results of the mutagenesis were verified by sequencing.

Expression and Purification of N-terminal Human TRPM3 Protein Constructs—Protein constructs Ala-35–Lys-124 and His-291–Gly-382 of the human TRPM3 ion channel were expressed as fusion proteins with thioredoxin and a His tag on the N terminus to increase their solubility in *Escherichia coli* Rosetta cells. Protein expression was induced by isopropyl-1-thio-β-D-galactopyranoside (Carl-Roth) for 12 h at 25 °C. The cells were pelleted by centrifugation and resuspended in 1× PBS buffer (pH 8.0) containing 1 M NaCl, 10 mM imidazole, 0.1 mM PMSF, 1 mM β-mercaptoethanol, and 0.05% Nonidet P-40. The cells were disrupted by sonication and centrifuged. The proteins were purified using affinity chromatography in a chelating Sepharose fast flow column (Amersham Biosciences) where 1× PBS buffer (pH 8.0) containing 0.5 M NaCl, 2 mM β-mercaptoethanol, and 400 mM imidazole was used for elution (see supplemental Fig. 1, *A* and *B*). Gel permeation chromatography in a Superdex 75 column (Amersham Biosciences) was used as a final purification step. The protein was eluted with 50 mM Tris-HCl buffer (pH 7.5) containing 250 mM NaCl, 2 mM β-mercaptoethanol, 0.05% Nonidet P-40, and 10% glycerol (see supplemental Figs. 1*B* and 2*B*). Protein samples were concentrated using spin columns for protein concentration (Millipore). Protein concentration was assessed by measuring absorption at 280 nm and by Bradford assay (16). The purity was verified using 15% SDS-polyacrylamide gel electrophoresis (PAGE). The integrity of the protein constructs was verified by MS analysis.

Mass Spectrometric Analysis—Two excised protein bands from SDS-PAGE, $TRPM3_{35-124}$ and $TRPM3_{291-382}$, were digested with trypsin endoprotease (Promega) directly in the gel after destaining and cysteine modification by iodoacetamide (17). The resulting peptide mixtures were extracted and loaded onto the MALDI-TOF/TOF target with α-cyano-4-hydroxycinnamic acid as the matrix, and positively charged spectra or MS/MS were acquired with an UltraFLEX III mass spectrometer (Bruker-Daltonics, Bremen, Germany) (see supplemental Fig. 3).

CaM Expression, Purification, and Labeling—CaM was expressed and purified as described previously (8). The protein was then dialyzed overnight into 10 mM $NaHCO_3$ (pH 10.0) at 4 °C. The protein sample was mixed with 0.6 M dansyl chloride (DNS) solution (Sigma) at a molar ratio of 1:1.5 and incubated at room temperature for 8 h. The sample was dialyzed overnight at 4 °C against 20 mM Tris-HCl buffer (pH 8.0) containing 250 mM NaCl and 2 mM $CaCl_2$ to remove the free dansyl chloride. The degree of protein labeling was checked by measuring the ratio of the fluorescence intensities of the unbound and bound states (excitation at 340 nm, emission at 500 nm).

S100A1 Cloning, Expression, Purification, and Labeling—cDNA coding the human S100A1 protein was cloned into the pET28b expression vector. The protein was expressed in BL21 *E. coli* cells. Protein expression was induced by isopropyl-1-thio-β-D-galactopyranoside (Carl-Roth) for 12 h at 25 °C. The cells were pelleted by centrifugation and resuspended in 50 mM Tris-HCl buffer (pH 7.5) containing 2 mM EDTA and 0.2 mM PMSF. The cells were disrupted by sonication and centrifuged. $CaCl_2$ was added to the supernatant (final concentration 5 mM). The protein was purified using affinity chromatography on phenyl-Sepharose CL4B (Amersham Biosciences), where 50 mM Tris-HCl buffer (pH 7.5) containing 1.5 mM EDTA and 100 mM NaCl was used for the elution. Gel permeation chromatography in a Superdex 75 column (Amersham Biosciences) was used as a final purification step. The protein was eluted with 50

TABLE 1

Calculated incidence (%) of secondary structures of CaM, $TRPM3_{35–124}$, and $TRPM3_{291–382}$ protein constructs and their complexes with CaM, determined by CD spectroscopy

	CaM	$TRPM3_{35–124}$	$TRPM3_{291–382}$	CaM/$TRPM3_{35–124}$ complex	CaM/$TRPM3_{291–382}$ complex
Helix	64	19	22	31	32
Antiparallel	4	12	11	9	9
Parallel	4	12	11	9	9
β-Turn	13	18	18	17	17
Random coil	16	39	38	34	33

TABLE 2

Calculated incidence (%) of secondary structures of S100A1, $TRPM3_{35–124}$, and $TRPM3_{291–382}$ protein constructs and their complexes with S100A1, determined by CD spectroscopy

	S100A1	$TRPM3_{35–124}$	$TRPM3_{291–382}$	S100A1/$TRPM3_{35–124}$ complex	S100A1/$TRPM3_{291–382}$ complex
Helix	66	19	22	36	35
Antiparallel	3	12	11	8	8
Parallel	3	12	11	8	8
β-Turn	12	18	18	16	17
Random coil	15	39	38	31	32

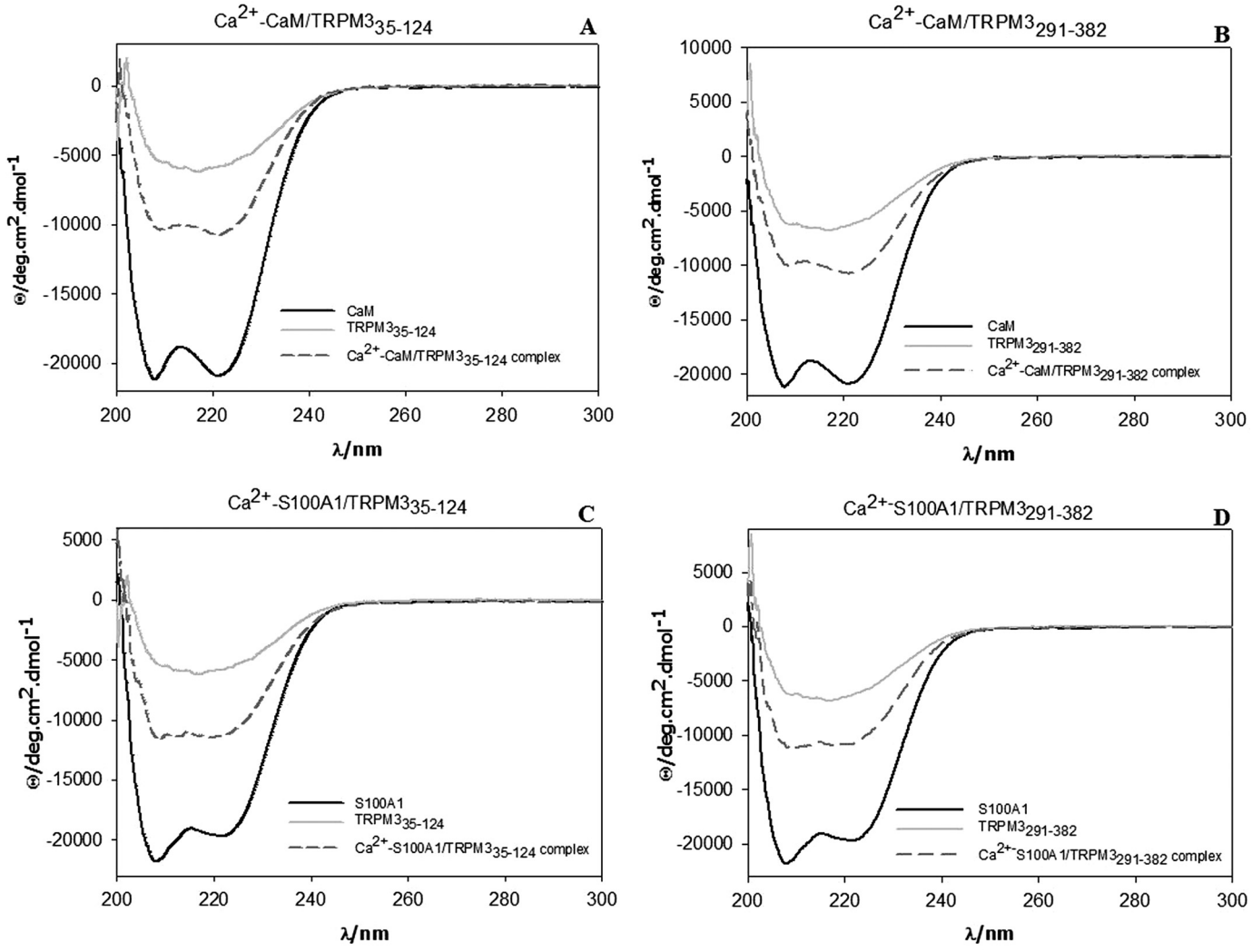

FIGURE 2. **CD spectra.** *A*, CaM, $TRPM3_{35–124}$ and CaM/$TRPM3_{35–124}$ complex. *B*, CaM, $TRPM3_{291–382}$ and CaM/$TRPM3_{291–382}$ complex. *C*, S100A1, $TRPM3_{35–124}$ and S100A1/$TRPM3_{35–124}$ complex. *D*, S100A1, $TRPM3_{291–382}$ and S100A1/$TRPM3_{291–382}$ complex. *Deg*, degree.

mM HEPES buffer (pH 7.0) containing 250 mM NaCl, 2 mM $CaCl_2$, 2 mM β-mercaptoethanol, and 10% glycerol. Protein samples were concentrated using spin columns for protein concentration (Millipore). Protein concentration was assessed by measuring absorption at 280 nm. The purity was verified using 15% SDS-PAGE. The protein was labeled with the fluorescent probe DNS, as described for CaM. The degree of protein labeling was checked by measuring the ratio of the fluorescence intensities of the unbound and bound states (excitation at 340 nm, emission at 500 nm).

TRPM3 $_{35-124}$	A K_D/μM	B K_d/μM
WT	1,29±0,14	0,198±0,018
K45A/R67A/R72A	4,80±1,32	0,290±0,088
K45A/R67A/K71A/R72A	8,04±0,43	0,339±0,044
R56A/K59A	4,93±0,91	0,295±0,079
R56A/K59A/K62A	5,69±1,25	0,482±0,110

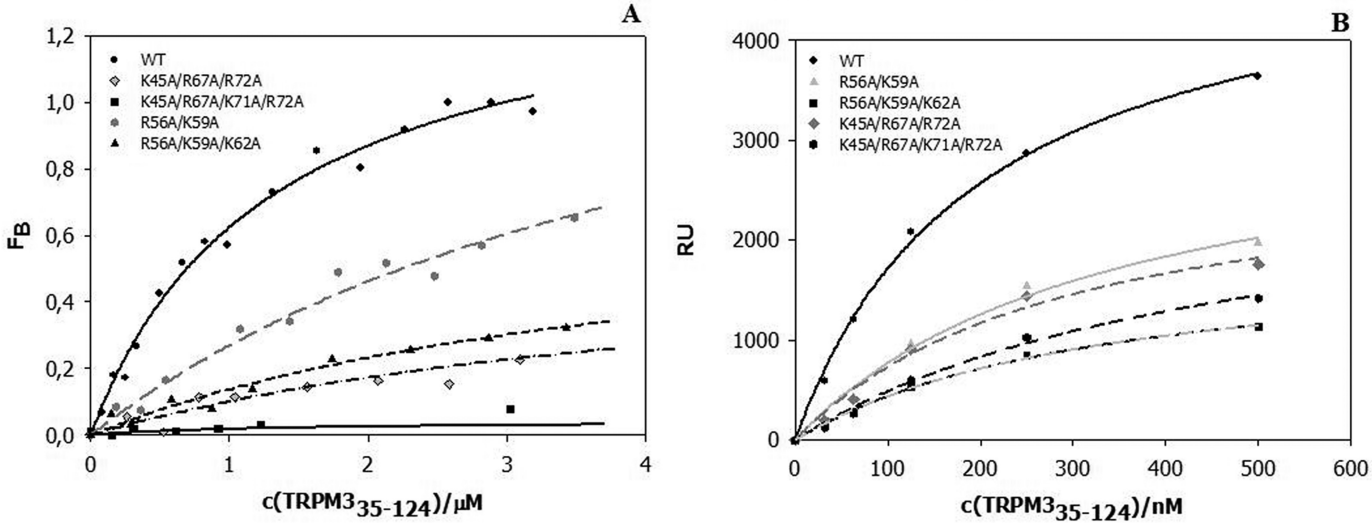

FIGURE 3. **Binding of CaM to TRPM3$_{35-124}$.** *Columns A* and *B*, summary of equilibrium dissociation constants obtained by steady-state fluorescence anisotropy measurement (*column A*) and dissociation constants obtained by SPR (*column B*). *A*, fluorescence anisotropy binding isotherms of wild type and mutants. *B*, SPR binding assay of wild type and mutants. *RU*, relative units.

TRPM3$_{35-124}$ and TRPM3$_{291-382}$-CaM and S100A1 Binding Assays—Steady-state fluorescence anisotropy measurements were performed on an ISS PC1™ photon counting spectrofluorometer at room temperature in a buffer containing 20 mM Tris-HCl (pH 7.5), 6 mM $CaCl_2$, and 5.4 mM DNS-CaM and DNS-S100A1, respectively. The samples were titrated with increasing amounts of a 200 μM solution of TRPM3 N-terminal protein constructs. At each TRPM3 concentration, the steady-state fluorescence anisotropy of DNS-CaM or DNS-S100A1 was recorded (excitation at 340 nm, emission at 500 nm). The fraction of bound TRPM3 protein (F_B) was calculated from Equation 1 (18)

$$F_B = (r_{obs} - r_{min})/[(r_{max} - r_{obs})Q + (r_{obs} - r_{min})] \quad \text{(Eq. 1)}$$

where Q represents the quantum yield ratio of the bound to the free form and was estimated by the ratio of the intensities of the bound to the free fluorophore. The parameter r_{max} is the anisotropy at saturation, r_{obs} is the observed anisotropy for any TRPM3 protein concentration, and r_{min} is the minimum observed anisotropy for the free CaM or S100A1. F_B was plotted against TRPM3 protein concentration and fitted using Equation 2 (18) to determine the equilibrium dissociation constant (K_D) for TRPM3$_{35-124}$/CaM, TRPM3$_{291-382}$/CaM, TRPM3$_{35-124}$/S100A1, and TRPM3$_{291-382}$/S100A1 complex formation.

$$F_B = \frac{K_D + [P_1] + [P_2] - \sqrt{(K_D + [P_1] + [P_2])^2 - 4[P_1][P_2]}}{2[P_1]} \quad \text{(Eq. 2)}$$

$[P_1]$ stands for the DNS-CaM or DNS-S100A1 concentration, and $[P_2]$ is the TRPM3 protein concentration. Nonlinear data fitting was performed using the program SigmaPlot 10.0. All experiments were carried out in at least triplicate. Control experiments with thioredoxin (Sigma-Aldrich) were performed to show that this protein is not involved in the binding to CaM or S100A1 in the fusion protein (data not shown).

To assess the role of Ca^{2+} on the binding of TRPM3 proteins to CaM and S100A1, we buffered Ca^{2+} present in the buffer after CaM and S100A1 purification with 10 mM EDTA. Then we performed the binding assays for the wild types of TRPM3$_{35-124}$ and TRPM3$_{291-382}$.

Surface Plasmon Resonance—Surface plasmon resonance (SPR) measurements were performed at 25 °C using a ProteOn XPR36 protein interaction array system (Bio-Rad). CaM and S100A1 proteins were diluted to concentrations of 5–50 μg/ml in 10 mM acetate buffer (pH 3.5) and immobilized on a GLC chip using a ProteOn amine coupling kit (Bio-Rad) at a flow rate of 30 μl/min. Nonreacted activated groups were blocked by the injection of 1 M ethanolamine (pH 8.5). The subsequent SPR measurements were carried out in Hanks' balanced salt buffer (10 mM HEPES, pH 7.4, 150 mM NaCl, 2 mM $CaCl_2$) enriched

TRPM3 $_{291-382}$	A K_D/μM	B K_d/μM
WT	0,92±0,17	0,481±0,074
K308A/R311A	4,08±1,68	0,520±0,078
K308A/R310A/R311A	$>>10^3$	$>>10^3$
K308A/R311A/K315A	$>>10^3$	$>>10^3$

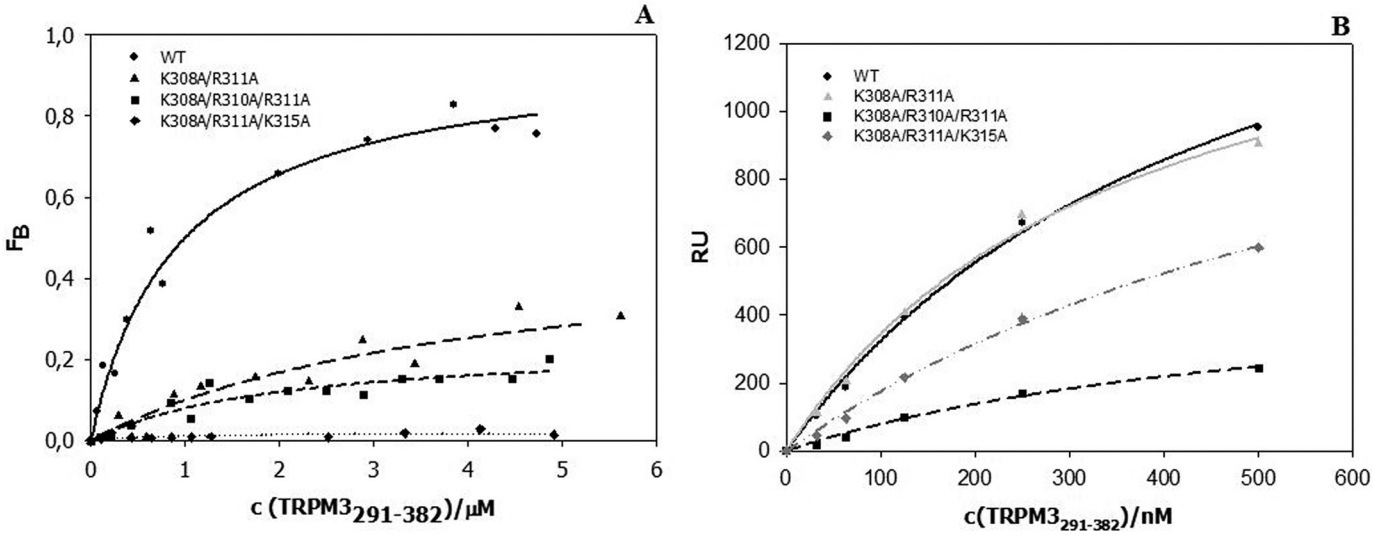

FIGURE 4. **Binding of CaM to TRPM3$_{291–382}$.** *Columns A* and *B*, summary of equilibrium dissociation constants obtained by steady-state fluorescence anisotropy measurement (*column A*) and dissociation constants obtained by SPR (*column B*). *A*, fluorescence anisotropy binding isotherms of wild type and mutants. *B*, SPR binding assay of wild type and mutants. *RU*, relative units.

with 0.005% Tween 20 at a flow rate of 25 μl/min for both the association and the dissociation phase of the sensorgrams. To determine the equilibrium binding, the association phases of five different concentrations of each analyte were brought to near equilibrium values (R_{eq}). Surfaces were typically regenerated with 200 μl of buffer containing 50 mM EDTA, 1 M NaCl, and 50 mM NaOH. Sensorgrams were evaluated using the ProteOn Manager software (Bio-Rad). Response curves were generated by subtracting the sensor background signal generated simultaneously in the "interspot" areas (those sites within the 6 × 6 array that were not exposed to ligand immobilization but were exposed to analyte flow). The background-subtracted curves were prepared for fitting by subtracting the signal generated simultaneously by buffer alone in the flow channel (5 test + 1 control channel). Assuming a Langmuir-type binding between the ligand (L) and analyte (A) (*i.e.* L + A ↔ LA), R_{eq} values were then plotted *versus* protein concentration (P_0), and the K_d value was determined by a nonlinear least squares analysis of the binding isotherm using the equation, $R_{eq} = r_{max}/(1 + K_d/P_0)$.

Circular Dichroism Spectroscopy—Circular dichroism (CD) experiments were carried out in a JASCO J-815 spectrometer (Tokyo, Japan). The peptide concentration was kept constant for all measured samples and was 0.35 mg/ml. The spectra were collected from 200 to 300 nm using a 0.1-cm quartz cell at room temperature. A 0.5-nm step resolution, 20 nm/min speed, 8 s response time and 1-nm bandwidth were used. After baseline correction, the final spectra were expressed as a molar ellipticity Θ (degrees cm^2/dmol) per residue. Secondary structure content was estimated using Dichroweb software (19).

Computer Homology Modeling—The sequences of human TRPM3 N terminus 41–70 and 304–324 were modeled via homology modeling using the program Modeller 9 version 5 (20). The structure of the voltage-gated calcium channel CaV1.2 IQ domain-Ca^{2+}-CaM complex (Protein Data Bank (PDB) code 2be6) (21), with a 63% sequence similarity, was used as a template for TRPM3 41–70, and the structure of the complex between CaM and αII-spectrin (PDB code 2fot) (22), with a 65% sequence similarity, was used for TRPM3 304–324. The sequences were aligned using CLUSTALX 2.0.10 (see Fig. 1) (23). The models were optimized by energy minimization using the GROMOS96 parameter set (24) (implementation of SwissPdbViewer (24)) and checked with ProSA-web (25, 26) for recognizing errors in the three-dimensional protein structure.

RESULTS

Purification and Expression of TRPM3$_{35–124}$ and TRPM3$_{291–382}$—We used the Calmodulin Target Database (15) to search for potential CaM binding motifs present in the intracellular termini of hTRPM3. Using our results from the database, we predicted two putative CaM binding sites in the regions 35–124 and 291–382 in the N terminus of the TRPM3. We cloned cDNA coding these regions into a suitable vector for protein expression in bacterial cells. To improve the solubility and expression yield of the proteins, we expressed and purified all the wild types and mutants as fusion proteins with the thiore-

TRPM3 $_{35-124}$	A K_D/μM	B K_d/μM
WT	1,43±0,37	0,304±0,037
K45A/R67A/R72A	5,66±0,27	5,300±0,157
K45A/R67A/K71A/R72A	>>10^3	>>10^3
R56A/K59A	4,04±1,22	3,500±0,085
R56A/K59A/K62A	5,96±0,33	4,800±0,124

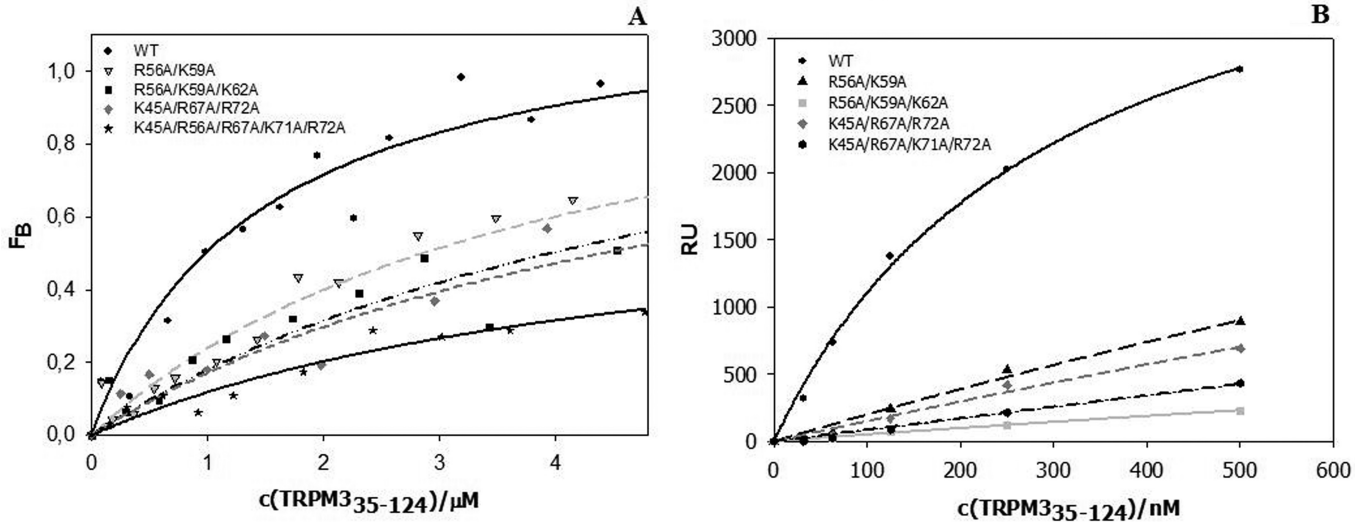

FIGURE 5. **Binding of S100A1 to TRPM3$_{35-124}$.** *Columns A* and *B*, summary of dissociation constants assessed by steady-state anisotropy measurement (*column A*) and SPR experiment (*column B*). *A*, fluorescence anisotropy binding isotherms of wild type and mutants. *B*, SPR binding assay of wild type and mutants. *RU*, relative units.

doxin tag and His_6 tag on their N terminus. All expressed fusion proteins were soluble and in sufficient amounts to perform the binding experiments. No interference between thioredoxin and the ligands was detected.

CD Spectroscopy—The secondary structure of the studied proteins was checked by CD spectroscopy (Fig. 1). Numerical analysis of the experimental spectra (19) enabled the relative abundance of the various secondary structures to be estimated (Tables 1 and 2). The α-helical conformation was found to be a major secondary structure component for CaM and S100A1 proteins, which is in good agreement with the conformation found in their native states. Although there is no known structure of the TRPM3 N terminus, the structural composition of both TRPM3 fusion proteins TRPM3$_{35-124}$ and TRPM3$_{291-382}$ is mostly an unordered structure, which is in a good agreement with the theoretical prediction based on their primary structure, suggesting that the proteins adopt their native fold. The experiment was also used to observe changes in secondary structural element composition during the creation of the TRPM3 fusion proteins/CaM or S100A1 complexes (Fig. 2). We compared the CD spectra of the complexes with the CD spectra of the proteins alone. Because the CD spectra of the mixture are the sum of the CD spectra for the TRPM3 protein constructs and CaM or S100A1 individually, this suggests that changes in the secondary structure of TRPM3$_{35-124}$ and TRPM3$_{291-382}$ have no significant influence on their binding to CaM or S100A1 (Fig. 2).

CaM Binds to Regions 35–124 and 291–382 on TRPM3 N Terminus—We used two different biophysical methods to test the binding of CaM to the potential binding sites. First, we employed steady-state fluorescence anisotropy measurements for both the wild types and the mutants (Figs. 3*A* and 4*A*). We titrated increasing amounts of TRPM3 protein constructs into a solution containing fluorescently labeled CaM. The equilibrium dissociation constant of the TRPM3$_{35-124}$/Ca^{2+}-CaM complex was estimated to be 1.29 ± 0.14 and 0.92 ± 0.17 μM for the TRPM3$_{291-382}$/Ca^{2+}-CaM complex. To further evaluate the binding sites, we investigated the role of some basic residues present within the binding domains. In the 35–124 region, the K45A/R67A/K71A/R72A mutation caused a 6-fold decrease in binding affinity to CaM. In the 291–382 region, both of the triple mutants K308A/R310A/R311A and K308A/R310A/K315A were unable to bind CaM.

To confirm the data obtained by steady-state fluorescence anisotropy, we used SPR as a different type of binding assay (Fig. 3*B* and 4*B*). CaM was bound covalently onto the chip, and the TRPM3 protein constructs and their mutants were washed over the chip. The dissociation constants of the TRPM3$_{35-124}$/Ca^{2+}-CaM and TRPM3$_{291-382}$/Ca^{2+}-CaM complex were estimated to be 0.198 ± 0.018 and 0.481 ± 0.074 μM, respectively. Mutations of the basic residues in TRPM3$_{35-124}$ caused an up to 4-fold decrease in binding affinity to CaM. The mutations K308A/R310A/R311A and K308A/R310A/K315A in TRPM3$_{291-382}$ resulted in a com-

$TRPM3_{291-382}$	A K_D/μM	B K_d/μM
WT	1,06±0,29	1,8±0,5
K308A/R311A	3,81±0,80	3,4±0,4
K308A/R310A/R311A	$>>10^3$	$>>10^3$
K308A/R311A/K315A	$>>10^3$	$>>10^3$

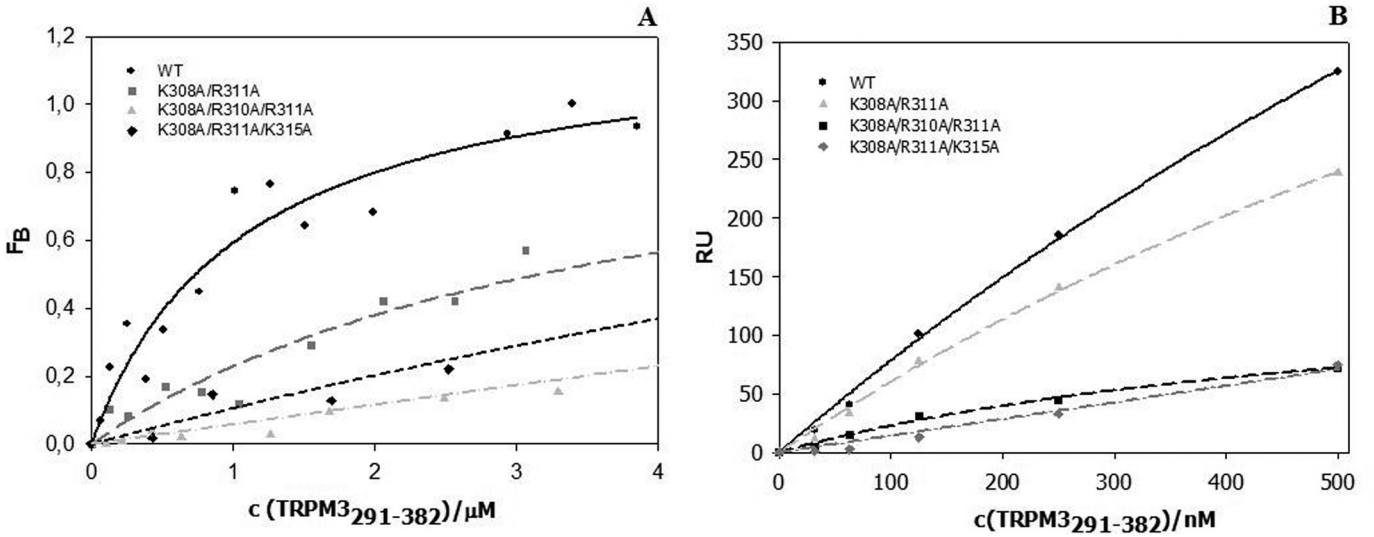

FIGURE 6. **Binding of S100A1 to $TRPM3_{291-382}$.** *Columns A* and *B*, summary of dissociation constants assessed by steady-state anisotropy measurement (*column A*) and SPR experiment (*column B*). *A*, fluorescence anisotropy binding isotherms of wild type and mutants. *B*, SPR binding assay of wild type and mutants. *RU*, relative units.

plete loss of binding affinity to CaM, as detected by fluorescence anisotropy.

S100A1 Binds to $TRPM3_{35-124}$ and $TRPM3_{291-382}$—As reviewed in previous studies, S100A proteins have been suggested to bind to similar structural motifs to CaM (11). Thus we used the same experimental approach to investigate whether the S100A1 protein is able to bind to $TRPM3_{35-124}$ and $TRPM3_{291-382}$ constructs in the same or a similar way to CaM. Equilibrium dissociation constants assessed by steady-state anisotropy measurement for the $TRPM3_{35-124}/Ca^{2+}$-S100A1 and $TRPM3_{291-382}/Ca^{2+}$-S100A1 complexes were estimated to be 1.43 ± 0.37 and 1.06 ± 0.29 μM, respectively (Figs. 5*A* and 6*A*). Dissociation constants determined by SPR for the $TRPM3_{35-124}/Ca^{2+}$-S100A1 and $TRPM3_{291-382}/Ca^{2+}$-S100A1 complexes were 0.304 ± 0.037 and 1.8 ± 0.5 μM, respectively (Figs. 5*B* and 6*B*). Mutant K45A/R67A/K71A/R72A of $TRPM3_{35-124}$ exhibited an inability to bind S100A1, and there was also no interaction detected for this mutant when measured by SPR. Both steady-state anisotropy measurement and SPR confirmed that triple mutations K308A/R310A/R311A and K308A/R310A/K315A caused a total loss of binding affinity for S100A1 in region 291–382 of the TRPM3 N terminus.

Binding of CaM and S100A1 to $TRPM3_{35-124}$ and $TRPM3_{291-382}$ Is Calcium-dependent—To determine the role of Ca^{2+} on CaM and S100A1 binding to regions 35–124 and 291–382 in the TRPM3 N terminus, we performed steady-state fluorescence anisotropy binding experiments in a solution lacking calcium (Fig. 7). We observed no increase in fluorescence anisotropy in either of the experiments, and thus we suggest that the binding is calcium-dependent.

CaM and S100A1 Compete for Overlapping Binding Sites in TRPM3 N Terminus—We mixed the CaM and S100A1 proteins in a 1:1 molar ratio with the $TRPM3_{35-124}$ and $TRPM3_{291-382}$ protein constructs. To investigate whether the complexes are able to bind CaM or S100A1, we carried out an SPR experiment. We gradually washed the $TRPM3_{35-124}/Ca^{2+}$-CaM, $TRPM3_{291-382}/Ca^{2+}$-CaM, $TRPM3_{35-124}/Ca^{2+}$-S100A1, and $TRPM3_{291-382}/Ca^{2+}$-S100A1 complexes over the CaM/S100A1 chip and observed the binding/nonbinding of the complexes to CaM or S100A1 (Fig. 6). Complexes of $TRPM3_{35-124}$ (Fig. 8*A*) and $TRPM3_{291-382}$ (Fig. 8*C*) with Ca^{2+}-CaM did not bind the S100A1 protein. Complexes of $TRPM3_{35-124}$ (Fig. 8*B*) and $TRPM3_{291-382}$ (Fig. 8*D*) with Ca^{2+}-S100A1 were not able to bind CaM. These data might imply that CaM and S100A1 bind to the same or overlapping binding sites within the TRPM3 N terminus.

Computer Homology Modeling—To visualize the interactions of the CaM binding sites on the TRPM3 N terminus with Ca^{2+}-CaM in more detail, we created computer homology models of the corresponding sequences. A structure of the ankyrin repeat domain on TRPV1 was reported to bind CaM (27), but no structure with this sequence was found in the complex with CaM. Thus we used the structures of other CaM binding peptides in complex with Ca^{2+}-CaM with a high degree of similarity. According to the secondary structure prediction, these sequences adopt the topology of an α-helix. We used other CaM binding peptides, namely the voltage-gated calcium channel CaV1.2 IQ domain (PDB code 2be6) and αII-spectrin (PDB code 2fot), as templates for our models. These templates have a high degree of sequence similarity with the

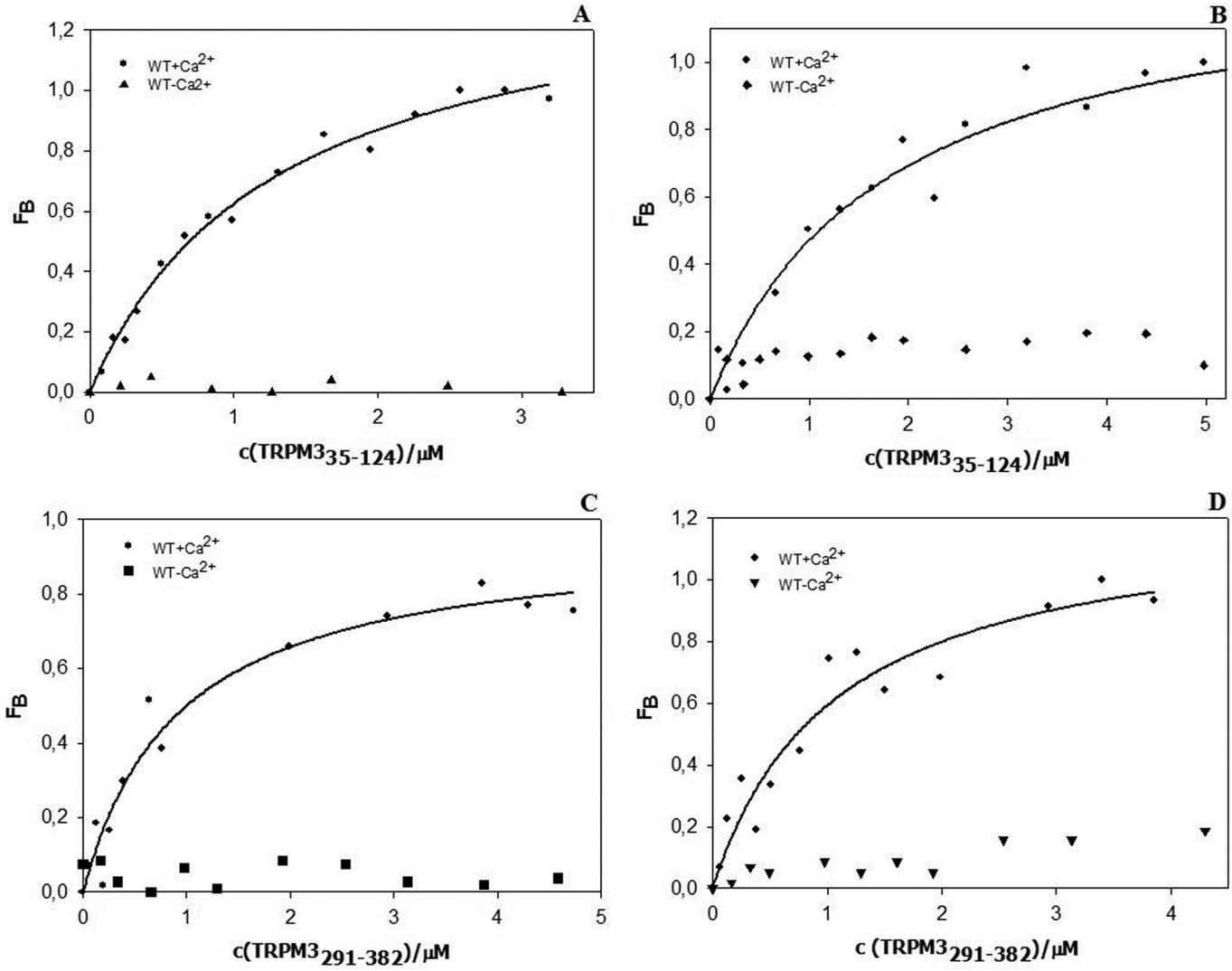

FIGURE 7. **Calcium-dependent binding of CaM and S100A1 proteins to $TRPM3_{35–124}$ and $TRPM3_{291–382}$.** *A*, CaM binding to $TRPM3_{35–124}$ in the presence (*circles*) and absence of calcium (*triangles*). *B*, S100A1 binding to $TRPM3_{35–124}$ in the presence (*circles*) and absence of calcium (*diamonds*). *C*, CaM binding to $TRPM3_{291–382}$ in the presence (*circles*) and absence of calcium (*squares*). *D*, S100A1 binding to $TRPM3_{291–382}$ in the presence (*circles*) and absence of calcium (*triangles*).

modeled sequences, especially in the positions of hydrophobic residues important for the interactions. Thus we modeled both the sequence 41–70 (Fig. 9*A*) and the sequence 304–324 (Fig. 9*B*) as α-helixes running through the central cavity of CaM, as was observed for the majority of such sequences. The model also suggested that basic residues could interact through ionic interactions with the negatively charged residues in CaM.

DISCUSSION

The TRPM3 ion channel has been proposed to play an important role in Ca^{2+} homeostasis serving as a Ca^{2+} entry pathway (2, 5). To date, no regulation via Ca^{2+}-binding proteins have been reported for this channel. CaM was shown to be an important regulator of various TRP ion channels, serving as both an activator and an inhibitor (7). The identification of more CaM binding sites was predicted from other TRP channels, and the functional implications of these interactions were suggested to be very complex, ranging from channel activation, facilitation, and inhibition/desensitization to subunit assembly, surface expression, recycling, and other regulation (7). It is known that the TRP channels are expressed without additional exogenous proteins. The channels require participation of endogenous signaling proteins for their activation and regulation (*e.g.* G_q protein, phospholipase C, CaM, protein kinases, and phosphatases).

Because Ca^{2+} and CaM are tightly linked, it is difficult to know whether CaM is involved in TRP channel activation or only in its inhibition. Furthermore, it is unclear whether these two processes act solely on the TRP channel or affect other stages of the signal transduction cascade (28).

Accordingly, TRPV1 channel expressed in *Xenopus* oocytes shows inhibition of the channel activity by Ca^{2+}. This effect is mediated by CaM as application of Ca^{2+}-CaM, but not of Ca^{2+} or CaM separately, inhibits the channel. In this system, no activating effects of either Ca^{2+}-CaM or Ca^{2+} were observed (29). In agreement with the inhibitory effects of Ca^{2+}-CaM, it has

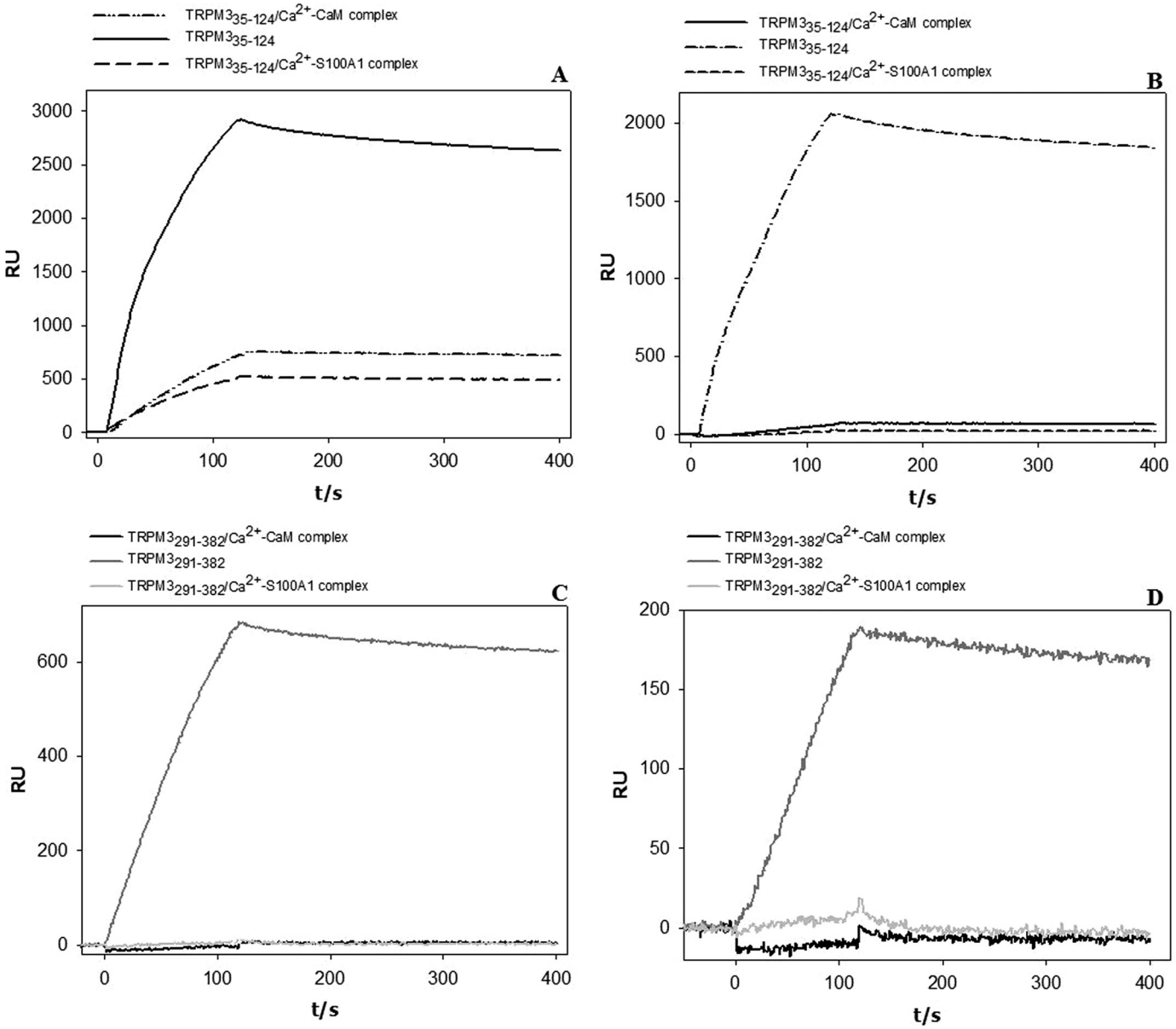

FIGURE 8. **SPR competition assay sensorgrams.** *A*, binding of TRPM3$_{35–124}$, TRPM3$_{35–124}$/Ca^{2+}-CaM and TRPM3$_{35–124}$/Ca^{2+}-S100A1 to S100A1. *RU*, relative units. *B*, binding of TRPM3$_{35–124}$, TRPM3$_{35–124}$/Ca^{2+}-CaM, and TRPM3$_{35–124}$/Ca^{2+}-S100A1 to CaM. *C*, binding of TRPM3$_{291–382}$, TRPM3$_{291–382}$/Ca^{2+}-CaM, and TRPM3$_{291–382}$/Ca^{2+}-S100A1 to S100A1. *D*, binding of TRPM3$_{291–382}$, TRPM3$_{291–382}$/Ca^{2+}-CaM, and TRPM3$_{291–382}$/Ca^{2+}-S100A1 to CaM.

been demonstrated that TRPC3 and TRPC4 are inhibited by Ca^{2+}-CaM but not by Ca^{2+} or CaM alone (7).

In the TRPM subfamily, CaM was demonstrated to be the Ca^{2+} sensor responsible for Ca^{2+}-dependent activation of TRPM2 via binding to the IQ motif present on the N terminus of this channel. Replacement of the motif disrupts the interaction of CaM and TRPM2, therefore abolishing TRPM2 activation evoked by Ca^{2+}. These results establish that Ca^{2+} is necessary and sufficient for TRPM2 activation and also elucidate that the Ca^{2+}-CaM binding to TRPM2 is required for Ca^{2+}-mediated TRPM2 activation. The data reveal a gating mechanism of TRPM2 and its alternative spliced isoforms that may represent a major gating mechanism *in vivo* and therefore confer novel, as yet unknown, physiological and/or pathological functions (30, 31). Moreover, five CaM binding sites were revealed on the N and C termini of TRPM4, and the three binding sites on the C-tail were suggested to be important for the Ca^{2+}-induced activation of this ion channel (32).

The aim of this study was to identify and characterize the putative CaM binding sites within the intracellular amino and carboxyl termini of TRPM3. We used two independent binding assays, steady-state fluorescence anisotropy measurement and SPR, to identify two CaM binding sites in regions Ala-35–Lys-124 and His-291–Gly-382 on the TRPM3 N terminus. These regions contain the 1-14, 1-10, and 1-5-10 consensus CaM recognition motifs with hydrophobic residues located in these positions (7), which is a common feature of CaM binding domains typically containing a basic amphiphilic α-helix, which can be classified into motifs based upon variations in the positions of conserved hydrophobic residues (14). We found several important basic residues in the N-terminal CaM bind-

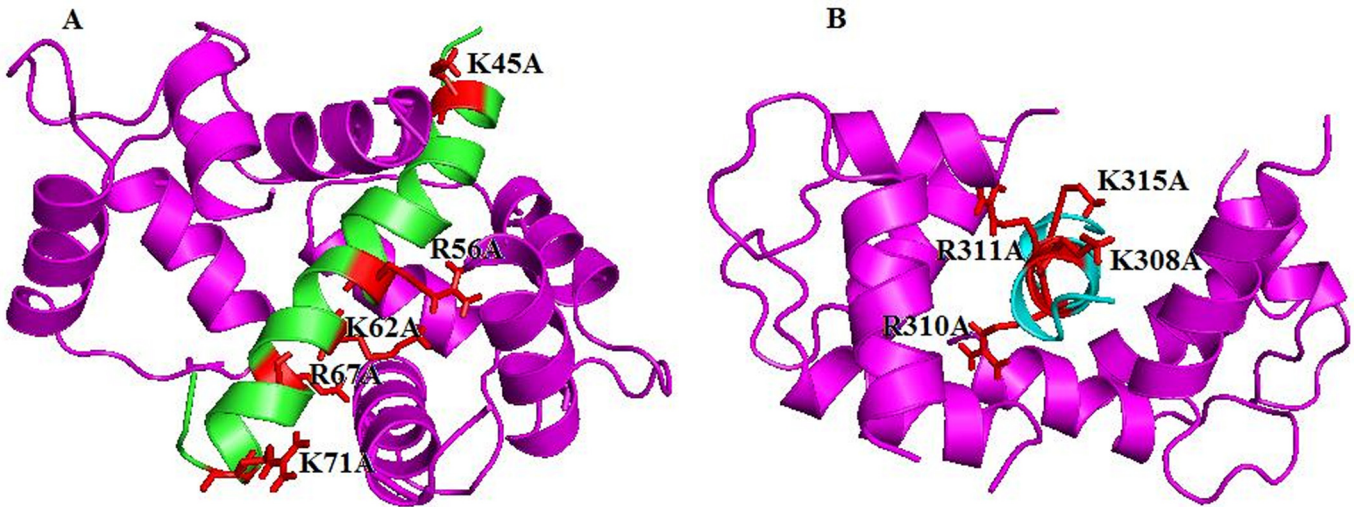

FIGURE 9. **Computer homology models of TRPM3 41–70 (*A*) and TRPM3 302–324 (*B*) with Ca^{2+}-CaM.**

ing domains, namely Lys-45, Arg-56, Lys-62, Arg-67, Lys-71, and Arg-72 on the $TRPM3_{35-124}$ and Lys-308, Arg-310, Arg-311, and Lys-315 on the $TRPM3_{291-382}$, which are crucial for CaM binding. Replacing these residues had a critical impact on the interaction, leading to a total loss of binding ability when three or more of these residues were replaced. The cluster of basic residues within the CaM binding motif was reported to interact with the negatively charged residues on CaM (33, 34), which was also found with the TRP channel family members TRPV1 (10), TRPV2 and TRPV5 (8).

The Ca^{2+}-binding S100 proteins were shown to interact with similar binding motifs to CaM (14, 35). Here we show that the S100A1 protein binds the same regions with equal affinity on the TRPM3 N terminus to CaM. Moreover, the mutation of positively charged residues within these domains affected the binding to S100A1, as was observed for CaM.

As was shown for the CaM binding sites present on the TRP channels, the binding of CaM to these sequences is calcium-dependent (7). To assess the role of calcium on CaM and S100A1 binding to the TRPM3 Ala-35–Lys-124 and His-291–Gly-382 N-terminal sequences, we performed the steady-state anisotropy measurement in a solution lacking calcium. We observed no changes in the anisotropy values, in contrast to the experiment when calcium was present, and thus we conclude that the binding is calcium-dependent.

To show that the binding sites for CaM/S100A1 on the TRPM3 N terminus overlap, we performed the SPR experiment. It is clear from the data that the complexes of the TRPM3 N-terminal constructs with Ca^{2+}-CaM do not bind S100A1, and similarly, the TRPM3 N-terminal complexes with Ca^{2+}-S100A1 do not bind CaM. A similar interaction was reported at the ryanodine receptor, where CaM and S100A1 compete for the same binding site with the same hydrophobic and basic residues being involved in CaM/S100A1 binding (36, 37). However, such evidence was missing for TRP channels, and here we show that the same basic residues participate in CaM/S100A1 binding.

To explain the interactions of the TRPM3 N-terminal CaM binding sites with CaM in detail, we created homology models of the sequences with CaM. According to the secondary structure prediction, the models are suggested to have the structure of an α-helix running through the central pore of CaM. We expect that the positively charged residues that we found to be crucial for CaM/S100A1 binding interact with the negatively charged residues in CaM.

Undoubtedly, CaM is a very important regulator of TRP channels, and it is therefore highly probable that, together with other Ca^{2+}-binding proteins, it could play an important role in the regulation of the TRPM3 ion channel via binding to its intracellular termini in the same way as was reported for other members of the TRPM subfamily. A possible role of Ca^{2+}-CaM in the gating mechanism was proposed for TRPM2 and TRPM4 (30, 31, 32) channels, and a similar way of regulation of TRPM3 could be assumed, but more functional studies will be required to elucidate the role of these Ca^{2+}-binding proteins in regulation of the channel.

Acknowledgments—We thank Dr. S. L. Hamilton from Baylor College of Medicine for providing us with rat CaM cloned into the pET3a vector and also Prof. C. Harteneck from the University of Tubingen for a clone of human TRPM3. We also thank Dr. L. Bednarova from the Institute of Organic Chemistry and Biochemistry of the Academy of Sciences of the Czech Republic for assistance with CD spectra measurements.

REFERENCES

1. Harteneck, C. (2005) Function and pharmacology of TRPM cation channels. *Naunyn Schmiedebergs Arch. Pharmacol.* **371,** 307–314
2. Lee, N., Chen, J., Sun, L., Wu, S., Gray, K. R., Rich, A., Huang, M., Lin, J. H., Feder, J. N., Janovitz, E. B., Levesque, P. C., and Blanar, M. A. (2003) Expression and characterization of human transient receptor potential melastatin 3 (hTRPM3). *J. Biol. Chem.* **278,** 20890–20897
3. Oberwinkler, J., Lis, A., Giehl, K. M., Flockerzi, V., and Philipp, S. E. (2005) Alternative splicing switches the divalent cation selectivity of TRPM3 channels. *J. Biol. Chem.* **280,** 22540–22548
4. Oberwinkler, J., and Phillipp, S. E. (2007). Trpm3. *Handb. Exp. Pharmacol.* 253–267
5. Grimm, C., Kraft, R., Sauerbruch, S., Schultz, G., and Harteneck, C. (2003) Molecular and functional characterization of the melastatin-related cat-

ion channel TRPM3. *J. Biol. Chem.* **278,** 21493–21501
6. Vriens, J., Owsianik, G., Hofmann, T., Philipp, S. E., Stab, J., Chen, X., Benoit, M., Xue, F., Janssens, A., Kerselaers, S., Oberwinkler, J., Vennekens, R., Gudermann, T., Nilius, B., and Voets, T. (2011) TRPM3 is a nociceptor channel involved in the detection of noxious heat. *Neuron* **70,** 482–494
7. Zhu, M. X. (2005) Multiple roles of calmodulin and other Ca^{2+}-binding proteins in the functional regulation of TRP channels. *Pflugers Arch.* **451,** 105–115
8. Holakovska, B., Grycova, L., Bily, J., and Teisinger, J. (2011) Characterization of calmodulin binding domains in TRPV2 and TRPV5 C-tails. *Amino Acids* **40,** 741–748
9. Friedlova, E., Grycova, L., Holakovska, B., Silhan, J., Janouskova, H., Sulc, M., Obsilova, V., Obsil, T., and Teisinger, J. (2010) The interactions of the C-terminal region of the TRPC6 channel with calmodulin. *Neurochem. Int.* **56,** 363–366
10. Grycova, L., Lansky, Z., Friedlova, E., Obsilova, V., Janouskova, H., Obsil, T., and Teisinger, J. (2008) Ionic interactions are essential for TRPV1 C terminus binding to calmodulin. *Biochem. Biophys. Res. Commun.* **375,** 680–683
11. Rezvanpour, A., and Shaw, G. S. (2009) Unique S100 target protein interactions. *Gen. Physiol. Biophys.* **28,** F39–F46
12. Rustandi, R. R., Baldisseri, D. M., Inman, K. G., Nizner, P., Hamilton, S. M., Landar, A., Landar, A., Zimmer, D. B., and Weber, D. J. (2002) Three-dimensional solution structure of the calcium-signaling protein apo-S100A1 as determined by NMR. *Biochemistry* **41,** 788–796
13. Wright, N. T., Varney, K. M., Ellis, K. C., Markowitz, J., Gitti, R. K., Zimmer, D. B., and Weber, D. J. (2005) The three-dimensional solution structure of Ca^{2+}-bound S100A1 as determined by NMR spectroscopy. *J. Mol. Biol.* **353,** 410–426
14. Rhoads, A. R., and Friedberg, F. (1997) Sequence motifs for calmodulin recognition. *FASEB J.* **11,** 331–340
15. Yap, K. L., Kim, J., Truong, K., Sherman, M., Yuan, T., and Ikura, M. (2000) Calmodulin Target Database. *J. Struct. Funct. Genomics* **1,** 8–14
16. Bradford, M. M. (1976) A rapid and sensitive method for the quantitation of microgram quantities of protein utilizing the principle of protein-dye binding. *Anal. Biochem.* **72,** 248–254
17. Prochazkova, K., Osicka, R., Linhartova, I., Halada, P., Sulc, M., and Sebo, P. (2005) The *Neisseria meningitidis* outer membrane lipoprotein FrpD binds the RTX protein FrpC. *J. Biol. Chem.* **280,** 3251–3258
18. Lakowicz, J. R. (2006) *Principles of Fluorescence Spectroscopy*, 3rd Ed., pp. 291–318, Springer, New York
19. Whitmore, L., and Wallace, B. A. (2008) Protein secondary structure analyses from circular dichroism spectroscopy: methods and reference databases. *Biopolymers* **89,** 392–400
20. Eswar, N., Webb, B., Marti-Renom, M. A., Madhusudhan, M. S., Eramian, D., Shen, M. Y., Pieper, U., and Sali, A. (2006) Comparative protein structure modeling using Modeller. *Curr. Protoc. Bioinformatics* Chapter 5, Unit 5.6
21. Van Petegem, F., Chatelain, F. C., and Minor, D. L., Jr. (2005) Insights into voltage-gated calcium channel regulation from the structure of the CaV1.2 IQ domain-Ca^{2+}/calmodulin complex. *Nat. Struct. Mol. Biol.* **12,** 1108–1115
22. Simonovic, M., Zhang, Z., Cianci, C. D., Steitz, T. A., and Morrow, J. S. (2006) Structure of the calmodulin αII-spectrin complex provides insight into the regulation of cell plasticity. *J. Biol. Chem.* **281,** 34333–34340
23. Larkin, M. A., Blackshields, G., Brown, N. P., Chenna, R., McGettigan, P. A., McWilliam, H., Valentin, F., Wallace, I. M., Wilm, A., Lopez, R., Thompson, J. D., Gibson, T. J., and Higgins, D. G. (2007) Clustal W and Clustal X version 2.0. *Bioinformatics* **23,** 2947–2948
24. Guex, N., and Peitsch, M. C. (1997) SWISS-MODEL and the Swiss-Pdb-Viewer: an environment for comparative protein modeling. *Electrophoresis* **18,** 2714–2723
25. Sippl, M. J. (1993) Recognition of errors in three-dimensional structures of proteins. *Proteins* **17,** 355–362
26. Wiederstein, M., and Sippl, M. J. (2007). ProSA-web: interactive web service for the recognition of errors in three-dimensional structures of proteins. *Nucleic Acids Res.* **35,** W407–W410
27. Lishko, P. V., Procko, E., Jin, X., Phelps, C. B., and Gaudet, R. (2007) The ankyrin repeats of TRPV1 bind multiple ligands and modulate channel sensitivity. *Neuron* **54,** 905–918
28. Minke, B., and Parnas, M. (2006) Insights on TRP channels from *in vivo* studies in *Drosophila*. *Annu. Rev. Physiol.* **68,** 649–684
29. Rosenbaum, T., Gordon-Shaag, A., Munari, M., and Gordon, S. E. (2004) Ca^{2+}/calmodulin modulates TRPV1 activation by capsaicin. *J. Gen. Physiol.* **123,** 53–62
30. Tong, Q., Zhang, W., Conrad, K., Mostoller, K., Cheung, J. Y., Peterson, B. Z., and Miller, B. A. (2006) Regulation of the transient receptor potential channel TRPM2 by the Ca^{2+} sensor calmodulin. *J. Biol. Chem.* **281,** 9076–9085
31. Du, J., Xie, J., and Yue, L. (2009) Intracellular calcium activates TRPM2 and its alternative spliced isoforms. *Proc. Natl. Acad. Sci. U.S.A.* **106,** 7239–7244
32. Nilius, B., Prenen, J., Tang, J., Wang, C., Owsianik, G., Janssens, A., Voets, T., and Zhu, M. X. (2005) Regulation of the Ca^{2+} sensitivity of the nonselective cation channel TRPM4. *J. Biol. Chem.* **280,** 6423–6433
33. Yamauchi, E., Nakatsu, T., Matsubara, M., Kato, H., and Taniguchi, H. (2003) Crystal structure of a MARCKS peptide containing the calmodulin-binding domain in complex with Ca^{2+}-calmodulin. *Nat. Struct. Biol.* **10,** 226–231
34. Matsuoka, Y., Hughes, C. A., and Bennett, V. (1996) Adducin regulation. Definition of the calmodulin-binding domain and sites of phosphorylation by protein kinases A and C. *J. Biol. Chem.* **271,** 25157–25166
35. Wilder, P. T., Lin, J., Bair, C. L., Charpentier, T. H., Yang, D., Liriano, M., Varney, K. M., Lee, A., Oppenheim, A. B., Adhya, S., Carrier, F., and Weber, D. J. (2006) Recognition of the tumor suppressor protein p53 and other protein targets by the calcium-binding protein S100B. *Biochim. Biophys. Acta* **1763,** 1284–1297
36. Prosser, B. L., Hernández-Ochoa, E. O., and Schneider, M. F. (2011) S100A1 and calmodulin regulation of ryanodine receptor in striated muscle. *Cell Calcium* **50,** 323–331
37. Wright, N. T., Prosser, B. L., Varney, K. M., Zimmer, D. B., Schneider, M. F., and Weber, D. J. (2008) S100A1 and calmodulin compete for the same binding site on ryanodine receptor. *J. Biol. Chem.* **283,** 26676–26683